Journal of Colloid and Interface Science 419 (2014) 79–85

Contents lists available at ScienceDirect

Journal of Colloid and Interface Science

www.elsevier.com/locate/jcis

A generalized diffusion model for growth of nanoparticles synthesized by colloidal methods

Tianlong Wen [1], Lucien N. Brush, Kannan M. Krishnan *

Department of Materials Science and Engineering, University of Washington, Box 352120, Seattle, WA 98195-2120, USA

ARTICLE INFO

Article history:
Received 10 September 2013
Accepted 7 December 2013
Available online 14 December 2013

Keywords:
Monodisperse colloidal nanoparticles
Diffusion controlled growth
Adsorption controlled growth
'Focusing' effect
Nanoparticle growth model
Nanoparticle synthesis
Diffusional layer

ABSTRACT

A nanoparticle growth model is developed to predict and guide the syntheses of monodisperse colloidal nanoparticles in the liquid phase. The model, without any *a priori* assumptions, is based on the Fick's law of diffusion, conservation of mass and the Gibbs–Thomson equation for crystal growth. In the limiting case, this model reduces to the same expression as the currently accepted model that requires the assumption of a diffusion layer around each nanoparticle. The present growth model bridges the two limiting cases of the previous model i.e. complete diffusion controlled and adsorption controlled growth of nanoparticles. Specifically, the results show that a monodispersion of nanoparticles can be obtained both with fast monomer diffusion and with surface reaction under conditions of small diffusivity to surface reaction constant ratio that results is growth 'focusing'. This comprehensive description of nanoparticle growth provides new insights and establishes the required conditions for fabricating monodisperse nanoparticles critical for a wide range of applications.

1. Introduction

Nanoparticle (NP) synthesis has been extensively explored for a large variety of materials ranging from metallic gold [1] to ionic iron oxide [2]. The extensive research in NP synthesis is due to its important role in improving many technologies and providing advances in fundamental research. For instance, a color display, comprised of semiconducting NPs (quantum dots), has been recently launched by Samsung Electronics [3]. NPs and their composites [4] have also been widely investigated for their unique thermal [5,6], electrical [7,8], magnetic [9–12] and optical [13,14] properties. In many applications, particularly in biomedicine [15], it is critical to process batches of NPs having narrow size distributions since their relaxation properties depend exponentially on their size. By fine tuning their size, CdSe NPs with a wide spectrum of colors can be obtained under UV radiation [16]. Magnetic blocking temperatures and hysteresis loops of magnetic NPs are affected by their size and distribution [4]. Further, NP self-assemblies allow us to understand the collective behavior of an ensemble of NPs and to explore performance of ensemble applications in nanoelectronics, bit patterned media [17,18], and nanoparticle lithography [19]. To obtain NP self-assembly with long-range order, their size distribution should be less than ~5% [20], otherwise self-assembled arrays may only exhibit short range order and contain many voids [21]. To this end, it is crucially important to experimentally explore synthetic routes under different conditions to obtain NPs with very narrow size distributions. It is also equally important to establish mathematical models of NP growth so that their preparation can be theoretically understood and directed.

A general strategy for chemically synthesizing monodisperse NPs is to separate the nucleation and growth stages of NP formation. LaMer and Dinegar proposed that there is a minimum degree of supersaturation of the nutrient species (monomers), $S_C = (C_C - C_0)/C_0$, where C_C and C_0 are the critical concentration for nucleation and solubility of the monomers, respectively. Below S_C, nucleation cannot occur even if the solution is in a supersaturated state [22]. By suddenly boosting monomer concentration above S_C, a prolific nucleation burst can be induced generating an abundance of nuclei in a very short period of time. The nucleation burst quickly consumes monomers bringing the concentration back down below S_C so that nucleation is halted leaving the surviving particles to continue growth. The process is shown in Fig. 1. By separating nucleation and growth, each nucleus is generated at almost the same time and thus all have nearly identical growth conditions. As a result, monodisperse NPs are produced. Later, it was proposed by Sugimoto that the NP size distribution could be either focused or broadened during growth depending upon the growth mechanism [23]. In their proposed model for NP growth, they assumed a diffusion layer of thickness, δ, due to Brownian motion [24] outside a growing NP. Absorption of monomers by growing NPs involves two steps. First, monomers move in the diffusion layer from the bulk solution toward the growing NPs;

* Corresponding author. Fax: +1 (206) 543 3100.
E-mail address: kannanmk@uw.edu (K.M. Krishnan).
[1] Present address: Department of Physics, Carnegie-Mellon University, USA.

0021-9797/$ - see front matter © 2013 Elsevier Inc. All rights reserved.
http://dx.doi.org/10.1016/j.jcis.2013.12.018

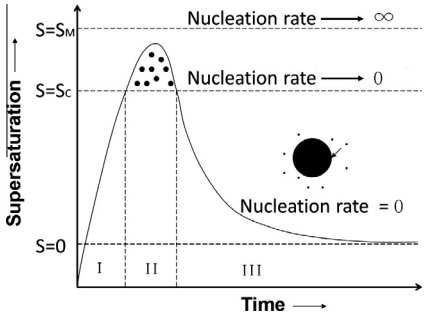

Fig. 1. Nucleation and growth as function of monomer supersaturation (adapted from Ref. [1]).

and second, these monomers are adsorbed by the growing NPs at the liquid/solid interface [23]. This mathematical model indicates that diffusion-controlled growth would result in monodisperse NPs while adsorption-controlled growth would lead to polydisperse NPs [23], which has been demonstrated in many NP preparations [25,26]. Without knowing the concentration profile of monomers in the diffusion layer and its relationship to its thickness, the growth model was developed upon an unfounded postulation. Many fundamentals and the underlying physics of NP growth are still ambiguous and questionable in this model. For example,

(1) Under what conditions, if any, is the assumption of such a diffusion layer outside a growing NP correct?
(2) Does the boundary of the concentration profile correspond to the physical boundary of the diffusion layer?
(3) What is the concentration profile in the diffusion layer outside a growing NP if the diffusion layer does exist?
(4) What defines the diffusion layer and how does its thickness affect or relate to other physical variables?

By addressing the above questions, NP growth can be better understood and thus NP synthesis can be better controlled. In this research work, without any prior assumptions, we start with the fundamental equations, i.e. the laws of diffusion, mass conservation and the Gibbs–Thomson equation for crystal growth [27], to build a mathematical model of NP growth. We show that there is no need to assume an arbitrary diffusion layer outside a NP in order to arrive at the same qualitative result in the limiting cases of diffusion-controlled and adsorption-controlled growth. Furthermore, the concentration profile outside a growing NP is calculated as a function of the monomer concentration in the bulk solution, the particle size, the diffusivity of the monomer, the adsorption coefficient, among other properties. Criteria for processing monodisperse NPs are discussed based upon the new mathematical model for NP growth. For simplicity, we follow Sugimoto's method and assume that the growing NPs are spherical in shape with radius R; for the cases considered here, the shape of the particle has only a minimal effect on its growth rate as discussed later.

2. NP growth model

For isotropic growth, in a spherical coordinate frame with the origin set at the center of the NP, Fick's second law of diffusion is given by:

$$\frac{\partial C}{\partial t} = D\left(\frac{\partial^2 C}{\partial r^2} + \frac{2}{r}\frac{\partial C}{\partial r}\right) \tag{1}$$

where C is the monomer concentration, that depends on time t and radial position r, and D is the diffusivity of monomer in the solution.

When the interface motion with respect to the origin of the coordinate frame (dR/dt) is slow compared to the time scale of monomer diffusion, the concentration profile around a NP is said to obey quasi-static conditions, namely, $\partial C/\partial t = 0$ for all r. In order for the quasi-static approximation to be valid the supersaturation of the monomer in solution ($C_b - C_0^\alpha$) should be much less than the difference in equilibrium concentrations of monomer between the NP and the solution ($C_0^\beta - C_0^\alpha$) (see Appendix 1 in Supplemental information 1), where C_b is the monomer concentration in the bulk solution. Here $C_0^\alpha \sim 0$, so that the quasi-static condition reduces to $C_0^\beta \gg C_b$, which is true in most cases. For example, in a typical cobalt NP synthesis by thermal decomposition, $C_b \sim 1.5 \times 10^2$ mol/m^3 before nucleation, while $C_0^\beta \sim 1.5 \times 10^5$ mol/m^3. Under quasi-static conditions, Fick's law of diffusion, Eq. (1), reduces to:

$$\frac{\partial^2 C}{\partial r^2} + \frac{2}{r}\frac{\partial C}{\partial r} = 0 \tag{2}$$

By considering the boundary condition at infinity ($C = C_b$ at $r = \infty$), the solution of the differential Eq. (2) is given by:

$$C = -\frac{A}{r} + C_b \tag{3}$$

where the constant A is a function (shown later) of particle size (R), diffusivity (D) and surface reaction constant (k). The concentration profile of Eq. (3) for a growing NP is schematically shown in Fig. 2(a).

During growth, the particle liquid/solid interface moves with a velocity, $v_n = dR/dt$ with respect to the center of the nanoparticle (Fig. 2a). Further, the rate of mass accumulation at the surface of a nanoparticle is equal to the total flux (per unit area) towards the nanoparticle, which gives [27]:

$$v_n[C_0^\beta - C_i] = -J_I = D_I \frac{\partial C}{\partial r}|_{r=R} \tag{4}$$

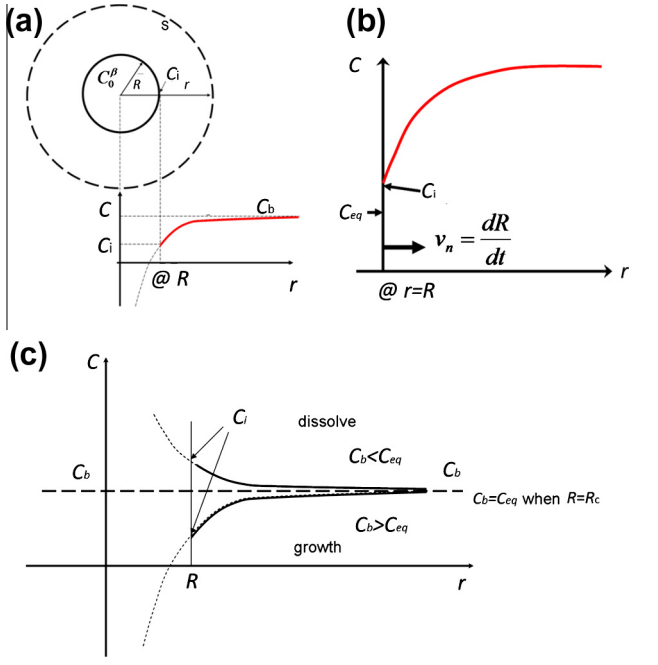

Fig. 2. (a) Concentration profile of monomers around a spherical nanoparticle of radius R, C_i and C_b are the concentrations at the interface and in the bulk, respectively. (b) Concentration profile in the solution, v_n is the interface velocity and C_{eq} is the equilibrium concentration of monomers in the solution at the surface of the nanoparticle, given by the Gibbs–Thomson equation. (c) Examples of concentration profiles in the solution for the cases in which $C_b < C_{eq}$ resulting in dissolution and for $C_b > C_{eq}$ resulting in growth.

where C_i is the monomer concentration at the interface, and J_I and D_I are the flux and diffusivity at the interface, respectively. If it is assumed that atom adsorption at the surface of the nanoparticle is linearly proportional to the interfacial supersaturation, J_I is given by:

$$-J_I = D^I \frac{\partial C}{\partial r}|_{r=R} = k(C_i - C_{eq}) \tag{5}$$

where C_{eq} is the equilibrium concentration of monomers at the surface of the nanoparticle, and k is the reaction constant. By combining Eqs. (4) and (5), C_i is given by:

$$C_i = \frac{\nu_n C_0^\beta + kC_{eq}}{k + \nu_n} \tag{6}$$

During steady-state growth, the total flux through any spherical surface, S, as denoted by the dashed line in Fig. 2(a), is given by Fick's first law of diffusion:

$$J_{tot} = 4\pi r^2 D \frac{dC}{dr} \tag{7a}$$

According to Eq. (3),

$$\frac{dC}{dr} = \frac{A}{r^2} \tag{7b}$$

By substituting Eq. (7b) into (7a), the total flux in the steady state is given by:

$$-J_{tot} = 4\pi r^2 D \frac{dC}{dr} = 4\pi r^2 D \frac{A}{r^2} = 4\pi DA \tag{7c}$$

which is independent of position. On the other hand, the total flux is related to the NP growth rate by:

$$-J_{tot} = \frac{4\pi R^2}{\Omega} \frac{dR}{dt} \tag{8}$$

where Ω is the volume of monomer. By equating Eqs. (7c) and (8), we get:

$$\frac{dR}{dt} = \frac{DA\Omega}{R^2}, \tag{9}$$

and substituting Eq. (9) into (6), the interface concentration is written as:

$$C_i = \frac{\frac{DA\Omega}{R^2} C_0^\beta + kC_{eq}}{\frac{DA\Omega}{R^2} + k} \tag{10}$$

At the interface ($r = R$), $C = C_i$, and by substituting Eq. (3) for C_i into Eq. (10), leads to an equation for the constant A:

$$\frac{D\Omega}{R^3}A^2 + \left[\frac{D\Omega}{R^2}(C_0^\beta - C_b) + \frac{k}{R}\right]A + k(C_{eq} - C_b) = 0 \tag{11a}$$

Under the quasi-static condition, $C_0^\beta \gg C_b$, and considering the fact that $\Omega = 1/C_0^\beta$, Eq. (11a) can be rewritten as:

$$\frac{D\Omega}{R^3}A^2 + \frac{D + kR}{R^2}A + k(C_{eq} - C_b) = 0 \tag{11b}$$

From which, constant A can be solved:

$$A = \frac{-\frac{D+kR}{R^2} + \sqrt{\left(\frac{D+kR}{R^2}\right)^2 + 4\frac{D\Omega}{R^3}k(C_b - C_{eq})}}{\frac{2D\Omega}{R^3}} \tag{12}$$

(Note that another solution of A is always negative and is thus abandoned). In Eq. (12) the denominator of A is always positive, so that the sign of A only depends on the bulk solution concentration (C_b) and the equilibrium concentration C_{eq}. Thus,

$$Sign(A) = \begin{cases} > & 0 \quad \text{for} \quad C_b < C_{eq} \\ = & 0 \quad \text{for} \quad C_b = C_{eq} \\ < & 0 \quad \text{for} \quad C_b < C_{eq} \end{cases} \tag{13}$$

The actual concentration (C_i) at the NP surface is between C_b and C_{eq}, and is weighted by ν_n and k according to Eq. (6). Depending on the sign of A, the concentration profile is plotted in Fig. 2(c). If the bulk solution concentration is larger than the equilibrium surface concentration (supersaturated), namely, $C_b > C_{eq}$, nanoparticles will grow; if $C_b < C_{eq}$, nanoparticles will dissolve; and if $C_b = C_{eq}$, nanoparticles are at their equilibrium size, which is the effective nucleus size of classical nucleation theory.

3. Discussion

3.1. Limiting cases of the diffusion and interface kinetic controlled growth

Eq. (12) can be rewritten as:

$$A = \frac{\frac{D+kR}{R^2}\left[\left(1 + \frac{4D\Omega kR(C_b - C_{eq})}{(D+kR)^2}\right)^{1/2} - 1\right]}{\frac{2D\Omega}{R^3}} \tag{14}$$

Under quasi-static approximation ($C_0^\beta \gg C_b$), $4D\Omega kR(C_b - C_{eq})/(D + kR)^2 \ll 1$ (see Appendix 2 in Supplemental information 2), so that the constant A simplifies to:

$$A = \frac{\frac{D+kR}{R^2} \times \frac{1}{2} \times \frac{4D\Omega kR(C_b - C_{eq})}{(D+kR)^2}}{\frac{2D\Omega}{R^3}} = \frac{kR^2(C_b - C_{eq})}{D + kR} \tag{15}$$

When the surface kinetics are fast ($D \ll kR$), the controlling step for particle growth is monomer diffusion towards the nanoparticle from the bulk solution. Under this condition, constant A is approximately equal to:

$$A \approx (C_b - C_{eq})R \tag{16}$$

By substituting Eq. (16) into (9), dR/dt can be calculated for diffusion controlled growth:

$$\frac{dR}{dt} = \frac{DA\Omega}{R^2} = \frac{D\Omega}{R^2}(C_b - C_{eq})R = \frac{D\Omega(C_b - C_{eq})}{R} \tag{17}$$

According to the Gibbs–Thomson equation for crystal growth [27], C_{eq} is equal to:

$$C_{eq} = C_\infty \exp\left(\frac{2\gamma\Omega}{Rk_BT}\right) \tag{18a}$$

whose first order expansion is:

$$C_{eq} = C_\infty\left(1 + \frac{2\gamma\Omega}{Rk_BT}\right) \tag{18b}$$

where γ and C_∞ are the specific surface energy and the equilibrium concentration of monomers at a flat surface, respectively. Accordingly, for a given bulk monomer concentration (C_b) there is a unique critical homogeneous nucleation size R_C:

$$C_b = C_\infty\left(1 + \frac{2\gamma\Omega}{R_Ck_BT}\right) \quad \Rightarrow \quad R_C = \frac{2\gamma\Omega}{k_BT(C_b - C_\infty)} \tag{18c}$$

that when substituted into (17), allows the growth rate of the nanoparticles to be written:

$$\frac{dR}{dt} = \frac{2D\gamma\Omega^2C_\infty}{k_BT}\frac{1}{R}\left(\frac{1}{R_C} - \frac{1}{R}\right). \tag{19}$$

In the limit that the interface kinetics are slow compared to the diffusion of monomers, ($D \gg kR$), the controlling step for particle growth is the monomer adsorption at the surface. Under this condition, the constant A in Eq. (14) can be reduced to:

$$A = \frac{kR^2(C_b - C_{eq})}{D} \tag{20}$$

By substituting Eq. (20) into (9), dR/dt can be obtained for interface adsorption controlled growth:

$$\frac{dR}{dt}=\frac{DA\Omega}{R^2}=\frac{D\Omega}{R^2}\times\frac{kR^2(C_b-C_{eq})}{D}=k\Omega(C_b-C_{eq}) \tag{21}$$

By substituting Eqs. (18b) and (18c) into (21), the growth rate can be calculated:

$$\frac{dR}{dt}=\frac{2k\gamma\Omega^2C_\infty}{k_BT}\left(\frac{1}{R_C}-\frac{1}{R}\right). \tag{22}$$

The growth rate of a nanoparticle by diffusion-controlled growth in Eq. (19) and adsorption-controlled growth in Eq. (22) are exactly the same as the results obtained in the mathematical model developed by Sugimoto [23], respectively. However, in this new mathematical model, no diffusion layer is assumed.

In Eqs. (19) and (22), when the particle size (R) is smaller (greater) than the critical size, R_c, the particle growth rate (dR/dt) is negative (positive) for both diffusion-controlled and adsorption-controlled growth, which means the particles will dissolve (grow) in both limiting cases. These results are consistent with the description of the effective nuclei size and the critical size in Fig. 2(c).

By differentiating the two sides of Eq. (19), and setting it equal to zero:

$$\frac{\partial(dR/dt)}{dR}=\frac{2D\gamma\Omega^2C_\infty}{k_BT}\left(-\frac{1}{R_CR^2}+\frac{2}{R^3}\right)=0, \tag{23}$$

the size of nanoparticle corresponding to the maximum growth rate is determined to be:

$$R=2R_c \tag{24}$$

The growth rate as a function of particle size is plotted for diffusion controlled growth in Fig. 3(a) revealing the maximum, and for adsorption controlled growth in Fig. 3(b) (note that there is no maximum growth rate for the case of interface controlled growth (adsorption controlled growth). As the particle grows larger its growth rate gradually increases).

For diffusion-controlled growth, after nucleation, an ensemble of NPs having a size just above the critical nucleation size, R_C will continue to grow. For particles in the size range, $R_C < R < 2R_C$, the growth rate of nanoparticles will quickly increase to the maximum at $2R_C$; then, larger growing nanoparticles will grow faster than smaller ones, broadening the size distribution. However, when the size of larger particles exceeds $2R_c$, their growth rate will quickly decrease, while the smaller nanoparticles will quickly grow more rapidly until they pass the $2R_C$ size threshold. After that, the growth rate of all NPs will slow down; however, the growth rate of larger particles remains slower than that of the smaller particles. In the ideal case, this process would result in all NPs having the same size and growth rate. As a result of the nucleation and growth kinetics, nearly monodisperse NPs can be obtained for diffusion-controlled growth. For adsorption-controlled growth on the other hand, the growth rate of larger NPs are always quicker than the smaller ones. As a result, only polydisperse NPs are obtained for adsorption-controlled growth.

3.2. Nanoparticle growth rate in the new model

NP growth rates given by Eqs. (19) and (22) represent the limiting cases of diffusion and adsorption controlled growth, respectively. By substituting A from Eq. (15) into (9), the growth rate of a nanoparticle is calculated to be:

$$\frac{dR}{dt}=\frac{DA\Omega}{R^2}=\frac{D\Omega(C_b-C_{eq})}{\frac{D}{k}+R} \tag{25}$$

which is valid for coupled interface- and diffusion-controlled growth thereby bridging the gap between these limiting cases. By substituting the Gibbs–Thomson equation into Eq. (25) then:

$$\frac{dR}{dt}=\frac{DA\Omega}{R^2}=\frac{D\Omega C_\infty\left(\exp\left(\frac{2\gamma\Omega}{R_Ck_BT}\right)-\exp\left(\frac{2\gamma\Omega}{Rk_BT}\right)\right)}{\frac{D}{k}+R} \tag{26}$$

Setting $n=2\gamma\Omega/k_BT$, then the general growth rate equation can be written as:

$$\frac{dR}{dt}=\frac{DA\Omega}{R^2}=\frac{D\Omega C_\infty\left(\exp\left(\frac{n}{R_C}\right)-\exp\left(\frac{n}{R}\right)\right)}{\frac{D}{k}+R} \tag{27}$$

To intuitively illustrate the effect of different parameters on the NP growth rate, consider a hypothetical system for which at a specific supersaturation, C_b, the critical nucleation size is $R_c\sim 2$ nm = 2×10^{-9} m. Using the representative values of $\gamma\sim 1$ J/m^2, $\Omega\sim(2\times10^{-10})^3=8\times10^{-30}$ m^3, for NP growth at high temperature, $T\sim 573$ K, so that $k_BT\sim 8\times10^{-21}$ J, then the index $n=2\gamma\Omega/k_BT\sim 2\times10^{-9}$ m. By substituting the values of n and R_c into Eq. (27), dR/dt can be plotted as a function of particle size, R, at different values of D/k in Fig. 4. The radii corresponding to the maximum growth rates are also plotted in green at different D/k ratios. Contrary to the simplified growth model given by Eq. (24) the radius of maximum growth rate is not twice the critical nucleation radius (R_c). Rather, it varies with parameters such as the D/k ratio. As the D/k ratio increases, the radius at the maximum growth rate moves to higher values.

As shown in Fig. 4, the D/k ratio can exponentially affect the growth rate of nanoparticles. Interestingly, when the D/k ratio is large (e.g. $D/k\geqslant 10R$ at $D/k=1000$ nm), the growth rate does not monotonously increase as predicted in Fig. 3(b). Rather, it slowly reaches its maximum growth rate at a large radius and then slowly decreases. It means that even under growth strongly affected by adsorption kinetics, the 'focusing' effect can still be achieved, albeit at a much larger particle size and at a slower rate. For NPs with final size smaller than R^*, the 'focusing' effect cannot be achieved before completion of particle growth, resulting in a polydisperse distribution of NP sizes. Here R^* is the radius of the particle at

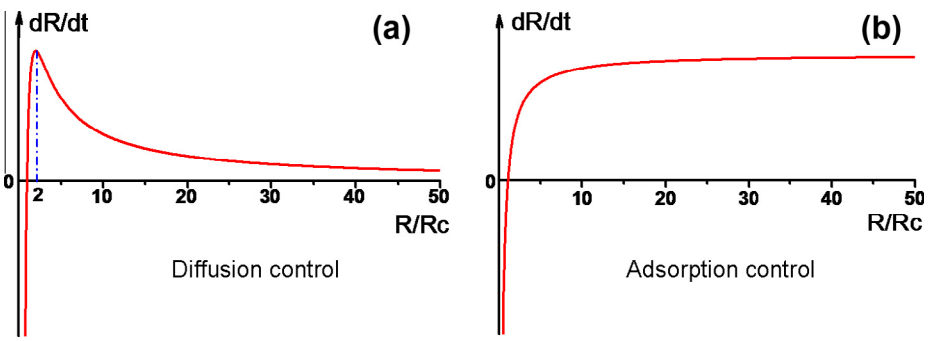

Fig. 3. Growth rate of nanoparticles as a function of particle size for diffusion controlled growth in (a) and adsorption controlled growth in (b).

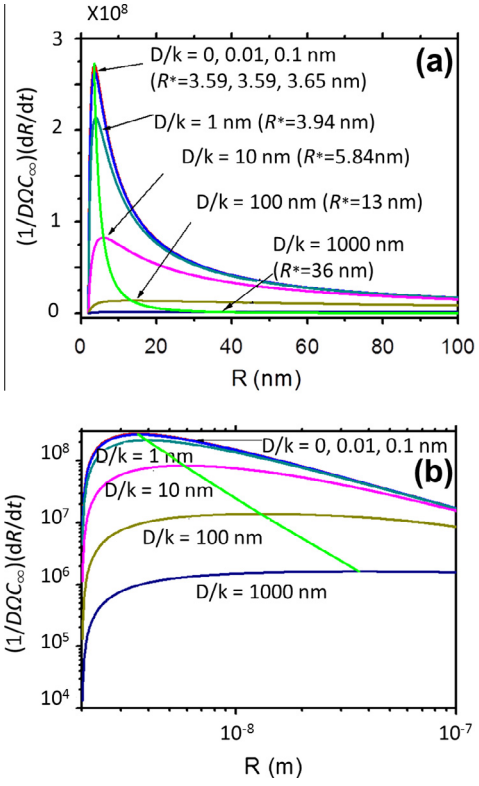

Fig. 4. Nanoparticle growth rate (normalized to $D\Omega C_\infty$) as a function of particle radius at different D/k ratio for a hypothetic system with $n = 2$ nm and $R_C = 2$ nm. The curves are plotted in linear scale in (a) and logarithmic scale in (b).

which the growth rate is maximum. However, for large NPs, the size 'focusing' effect might also be achieved over an extended period of time and at a slower growth rate, which is applicable in the case of large monodisperse colloidal particles, such as silica nano spheres [28].

To achieve efficient 'focusing', according to Fig. 4, R^* should be minimized while the growth rate, $(dR/dt)_{max}$ should be maximized. Minimizing R^* and maximizing $(dR/dt)_{max}$ corresponds to maximizing the slopes of dR/dt with respect to R before and after the maximum growth rate is achieved, respectively. Under this condition, the ensemble of NP nuclei can grow rapidly and finish the defocusing stage at $R_c < R < R^*$ and the 'focusing' stage at $R > R^*$ can start as early as possible. This is extremely important for NPs with small final size. In addition, under this condition, the negative slope of dR/dt with respect to R at $R > R^*$ is very large after $(dR/dt)_{max}$ is achieved. As a result, the growth rate of larger NPs will quickly slow down for $R > R^*$, while the growth rate of smaller NPs will still be rapid thereby achieving an effective 'focusing' dynamics. These two conditions can be achieved by decreasing the D/k ratio and increasing the diffusivity D. *A key finding of this work is that to make monodisperse NPs, monomer diffusion and surface reaction should be rapid while maintaining a small D/k ratio.*

For larger values of specific surface energy, the magnitude of n increases in Eq. (27) as well. Fig. 5(a) and (b) is plots of the normalized growth rate as a function of particle radius at a fixed D/k ratio (=1 nm) for different values of the n index. The maximum growth rate and the corresponding radii are also plotted as a function of n in Fig. 5(c) and (d) for $D/k = 1$ nm and 100 nm, respectively. As n increases, the maximum growth rate increases exponentially and the corresponding radius decreases at the same time. The trend is the same as for the case in which the D/k ratio is varied as shown in Fig. 5(d). According to the two criteria, for an efficient 'focusing' effect, a large n index should result in a monodisperse NP ensemble. The surface energy of a *growing* nanoparticle can be modified by using a surface surfactant coating although this is a complicated procedure in practice. This is part of the reason that surfactants play a crucial role in practical NP synthesis [29]. This will also affect the NP growth according to Fig. 5. When the surface energy is anisotropic, corners and/or facets may appear because shapes with these features lower the overall surface energy of the system [30] compared to spherical particles. In addition, surfactant coatings would also affect the interface attachment and reaction kinetics. Stronger binding between NP surface and functional groups of surfactants will make it less efficient for adsorption of monomers, resulting in larger D/k value. This, according to Fig. 4, will result in slower growth rate and thus smaller nanoparticles. It will also make it less efficient to make monodisperse nanoparticles.

Finally, as the temperature T increases, n will decrease by a factor of less than one while the diffusivity will increase according to Einstein–Stokes equation. At the same time, as the temperature increases, the monomer concentration is often much higher due to the temperature assisted generation of monomers (due to the decomposition of organometallic precursors [31]). A higher monomer concentration can make nucleation much easier, by creating a smaller effective nucleation size, R_c. Fig. 6(a) shows the normalized NP growth rate as a function of particle size for different effective nucleation sizes. The maximum growth rate and the corresponding radius are also plotted as a function of nuclei size in Fig. 6(b). As shown in Fig. 6(a), when effective nucleation size decreases from 1 nm to 0.5 nm, the normalized maximum growth rate of nanoparticle increases by a factor of ~15, and the radius corresponding to the maximum growth rate decreases by a factor of ~2. According to Fig. 6(b), the maximum growth rate decreases exponentially and the corresponding radius increases linearly as the effective nucleation size increases. As a result, decreasing the effective nuclei size (or increasing the monomer concentration) is an effective way to achieve the 'focusing' effect during the growth of nanoparticles. However, at the same time, the monomer concentration should be kept low relative to the critical supersaturation (S_c) for nucleation as shown in Fig. 1 to prevent secondary nucleation events from occurring. For optimal growth conditions leading to monodisperse NPs, the monomer concentration should be kept as high as possible without inducing secondary nucleation, as shown by the curve[2] d (red) in Fig. 7. Monodisperse iron oxide nanoparticles are often synthesized by methods developed by Sun group [32], Hyeon group [33] and Colvin group [34]. Among them, iron oxide nanoparticles synthesized by Colvin method usually have highest monodispersity. It can be attributed to the continuous generation of iron oleate by reaction between FeOH and oleic acid at high temperature, which keeps the precursor (iron oleate) concentration high at the growth stage. Another method is to continuously and slowly inject precursor to ensure high concentration of monolayer at the growth stage of nanoparticles.

4. Conclusions

In summary, a model of nanoparticle growth at low supersaturation, under the combined effects of monomer diffusion and local interface adsorption kinetics is presented. The growth model is formulated without any *a priori* assumptions concerning the diffusion processes. The limiting cases of growth controlled entirely by diffusion and growth controlled entirely by monomer adsorption reduce to previously derived models that were built upon an ad hoc approximation for the diffusion layer surrounding a growing nano-

[2] For interpretation of color in Fig. 7, the reader is referred to the web version of this article.

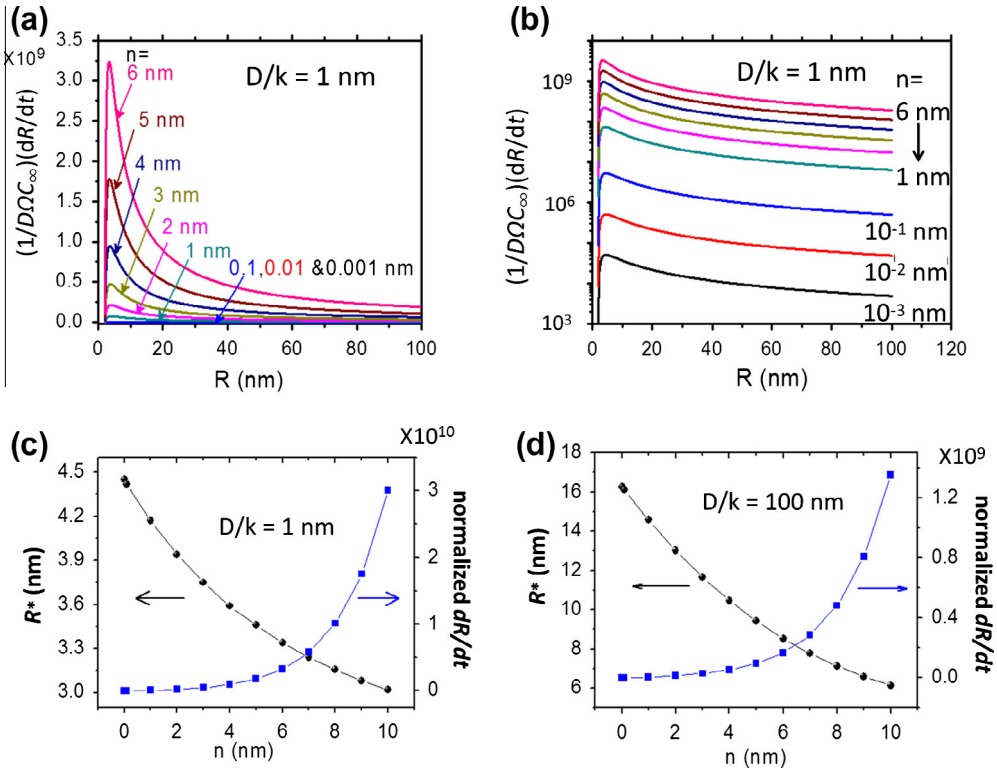

Fig. 5. (a) Nanoparticle growth rate (normalized to $D\Omega C_\infty$) as a function of particle radius for $D/k = 1$ nm and $R_c = 2$ nm for different values of n. (b) The same plot is also shown in a logarithmic scale. (c) The maximum growth rate and corresponding radius are plotted as a function of n index at $D/k = 1$ nm. (d) The same plot as in (c) but for $D/k = 100$ nm.

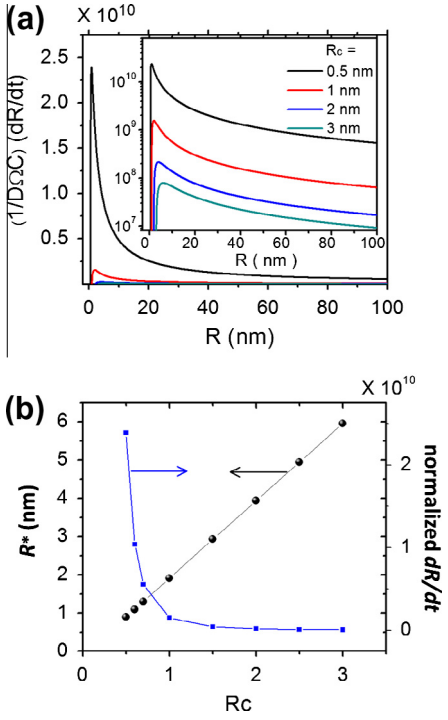

Fig. 6. (a) Nanoparticle growth rate (normalized to $D\Omega C_\infty$) as a function of particle radius for $D/k = 1$ nm at different critical nucleation radii (R_c). The inset in (a) is the same plot on a logarithmic scale. (b) The maximum growth rate and corresponding radius are plotted as a function of R_c at $D/k = 0$.

particle. In the model presented in this work, the gap is bridged between complete interface controlled growth and diffusion controlled growth, and as a result leads to new insight into

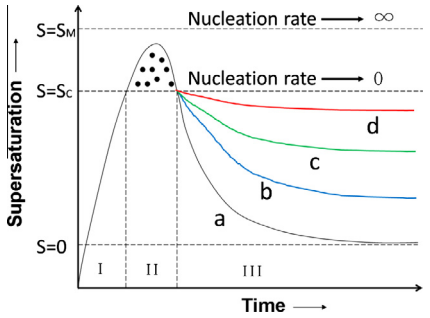

Fig. 7. Different supersaturation levels (represented by curve a, b, c and d in the figure) of monomers at growth stage (stage III). Higher supersaturation level benefits growth of monodisperse nanoparticles.

nanoparticle growth process. Results show that a monodispersion of nanoparticles can be obtained both with fast monomer diffusion and with surface reaction under conditions of small diffusivity to surface reaction constant ratio that results is growth 'focusing'. In addition, the focusing effect can also be affected by the specific surface energy of a growing NPs and the effective nucleation size, which are manipulated by adding surfactant to the solution. We expect this model to give a comprehensive prediction of NP growth and thus help enable tuning of experimental conditions for the production of monodisperse NPs.

Acknowledgment

This Project is partially supported by National Science Foundation DMR #0501421.

Appendix A. Supplementary material

Supplementary data associated with this article can be found, in the online version, at http://dx.doi.org/10.1016/j.jcis.2013.12.018.

References

[1] M. Brust, M. Walker, D. Bethell, D.J. Schiffrin, R. Whyman, J. Chem. Soc. Chem. Commun. (1994) 801–802. http://pubs.rsc.org/en/Content/ArticleLanding/1994/C3/c39940000801#!divAbstract.
[2] T. Hyeon, S.S. Lee, J. Park, Y. Chung, H.B. Na, J. Am. Chem. Soc. 123 (2001) 12798–12801.
[3] T.H. Kim, K.S. Cho, E.K. Lee, S.J. Lee, J. Chae, J.W. Kim, D.H. Kim, J.Y. Kwon, G. Amaratunga, S.Y. Lee, B.L. Choi, Y. Kuk, J.M. Kim, K. Kim, Nat. Photonics 5 (2011) 176–182.
[4] T. Wen, K.M. Krishnan, J. Phys. D: Appl. Phys. 44 (2011) 393001.
[5] P. Buffat, J.P. Borel, Phys. Rev. A 13 (1976) 2287–2298.
[6] T. Wen, K.M. Krishnan, J. Phys. Chem. C 114 (2010) 14838–14842.
[7] C.T. Black, C.B. Murray, R.L. Sandstrom, S.H. Sun, Science 290 (2000) 1131–1134.
[8] T. Wen, D. Liu, C.K. Luscombe, K.M. Krishnan, Appl. Phys. Lett. 95 (2009) 082509.
[9] T. Wen, W. Liang, K.M. Krishnan, J. Appl. Phys. 107 (2010) 09B501. http://scitation.aip.org/content/aip/journal/jap/107/9/10.1063/1.3350901.
[10] R.H. Kodama, J. Mag. Mag. Mater. 200 (1999) 359–372.
[11] T. Wen, K.M. Krishnan, J. Appl. Phys. 109 (2011) 07B515. http://scitation.aip.org/content/aip/journal/jap/109/7/10.1063/1.3544493.
[12] S.A. Majetich, T. Wen, T.O. Mefford, MRS Bull. 38 (2013) 899–903.
[13] K.L. Kelly, E. Coronado, L.L. Zhao, G.C. Schatz, J. Phys. Chem. B 107 (2003) 668–677.
[14] A.N. Shipway, E. Katz, I. Willner, Chem. Phys. Chem. 1 (2000) 18–52.
[15] Kannan M. Krishnan, IEEE Trans. Mag. 46 (2010) 2523–2558.
[16] D.J. Norris, M.G. Bawendi, Phys. Rev. B 53 (1996) 16338–16346.
[17] S.A. Majetich, T. Wen, R.A. Booth, ACS Nano 5 (2011) 6081–6084.
[18] M.T. Moneck, J.G. Zhu, Dekker Encyclopedia of Nanoscience and Nanotechnology, second ed., Taylor & Francis, 2013. http://www.tandfonline.com/doi/abs/10.1081/E-ENN2-120049358#.UsNDDLQbA38.
[19] T. Wen, R.A. Booth, S.A. Majetich, Nano Lett. 12 (2012) 5873–5878.
[20] C.B. Murray, C.R. Kagan, M.G. Bawendi, Annu. Rev. Mater. Sci. 30 (2000) 545–610.
[21] T. Wen, S.A. Majetich, ACS Nano 5 (2011) 8868–8876.
[22] V.K. LaMer, R.H. Dinegar, J. Am. Chem. Soc. 72 (1950) 4847–4854.
[23] T. Sugimoto, Adv. Colloid Interface Sci. 28 (1987) 65–108.
[24] T. Sugimoto, AlChe J. 24 (1978) 1125–1127.
[25] X. Peng, J. Wickham, A.P. Alivisatos, J. Am. Chem. Soc. 120 (1998) 5343–5344.
[26] J. Park, J. Joo, S.G. Kwon, Y. Jang, T. Hyeon, Angew. Chem. Int. Ed. 46 (2007) 4630–4660.
[27] D.A. Porter, K.E. Easterling, Phase Transformation in Metals and Alloy, second ed., Chapman and Hall, 1992.
[28] W. Stöber, A. Fink, E. Bohn, J. Colloid Interface Sci. 26 (1968) 62–69.
[29] Y. Bao, W. An, H.C. Turner, K.M. Krishnan, Langmuir 26 (2010) 478.
[30] M.L. Personick, M.R. Langille, J. Zhang, N. Harris, G.C. Schatz, C.A. Mirkin, J. Am. Chem. Soc. 133 (2011) 6170–6173.
[31] V.F. Puntes, K.M. Krishnan, P.A. Alivisatos, Science 291 (2001) 2115.
[32] S. Sun, H. Zeng, D.B. Robinson, S. Raoux, P.M. Rice, S.X. Wang, G. Li, J. Am. Chem. Soc. 126 (2004) 273–279.
[33] J. Park, K. An, Y. Hwang, J.G. Park, H.J. Noh, J.Y. Kim, J.H. Park, N.M. Hwang, T. Hyeon, Nat. Mater. 3 (2004) 891–895.
[34] W.W. Yu, J.C. Falkner, C.T. Yavuz, V.L. Colvin, Chem. Commun. (2004) 2306–2307. http://pubs.rsc.org/en/Content/ArticleLanding/2004/CC/B409601K#!divAbstract.